Crystallization Kinetics in Mixtures of Poly(vinylidene fluoride) and Poly(methyl methacrylate): Two-Step Diffusion Mechanism

Hiromu Saito, Tetsuo Okada, Toshihiko Hamane, and Takashi Inoue*

Department of Organic and Polymeric Materials, Tokyo Institute of Technology, Ookayama, Meguro-ku, Tokyo 152, Japan

Received December 14, 1990

ABSTRACT: We investigated the spherulite growth rate, G, in mixtures of poly(vinylidene fluoride) (PVDF) and poly(methyl methacrylate) (PMMA) at various crystallization temperatures, T_c. The molecular weight of PMMA, M_2, was changed in a wide range ($1.3 < 10^{-4}M_2 < 93$). As T_c increased, a regime transition from II to I was found to occur. At the regime transition temperature, an abrupt drop in G was observed. In regime I, G strongly depended on M_2, while there was a weak dependence in regime II. A systematic regime transition, III → II → I, was found to occur as the volume fraction of PMMA, ϕ_2, increased. The PMMA blend with larger M_2 exhibited the regime transition at smaller ϕ_2. These results were successfully interpreted by the modified Hoffman-Lauritzen theory involving the two-step diffusion mechanism characteristic of the crystallization of a polymer blend, i.e., the mutual-diffusion process for the formation of the first stem at the crystal surface and the self-diffusion process for the attachment of following stems in the chain.

Introduction

It is well-known that the crystallization rate of a crystalline polymer is reduced by mixing it with amorphous polymer. Typical examples are seen in poly(vinylidene fluoride) (PVDF)/poly(methyl methacrylate) (PMMA),[1] poly(caprolactone)/poly(vinyl chloride),[2] PVDF/poly(ethyl acrylate),[3] and poly(ethylene oxide)/PMMA[4] systems. As in the case of neat crystalline polymer systems, the growth rate in the crystalline/amorphous polymer blends has been formulated by the Hoffman-Lauritzen theory,[5] with minor modifications in the melting point depression with mixing and in the reduction of chain mobility by blending the high T_g component.[1-4]

However, from a microscopic point of view, the crystallization behavior in the mixtures is expected to be essentially different from that of the neat systems. In the mixtures, the amorphous polymer should diffuse away from a crystal growth front; i.e., the exclusion should take place in an order of lamella size, at least. It will result in complicated diffusion so that the crystallization kinetics would differ from that of the neat systems. So far, such an exclusion effect has not been taken into account in the crystallization kinetics.

Experimentally, the exclusion effect will be elucidated by investigating the effect of the molecular weight of the amorphous polymer on the crystallization rate. Hence, in this article, we prepare a series of PMMA specimens having different molecular weights in a wide range and investigate the growth rate of PVDF/PMMA blends. The kinetic study is carried out in a wide temperature range to verify the applicability of the Hoffman-Lauritzen theory. We undertake a quantitative analysis of the kinetic results.

Experimental Section

The polymer specimens used in this study and their characteristics are shown in Table I. PVDF and PMMA were dissolved at 5 wt % total polymer in *N,N*-dimethylacetamide. The solution was cast on a glass plate, and the solvent was evaporated under a reduced atmosphere of 10^{-2} mmHg at room temperature. The case film was further dried under vacuum (10^{-4} mmHg) at room temperature for 2 days.

The specimen was held at 200 °C for 10 min. Then the melt underwent a rapid quench to the crystallization temperature by putting it in a hot stage (Linkam TH600 heating-cooling stage, Linkam Scientific Instruments, Ltd.) set on the optical microscope stage and was crystallized isothermally.

The time variation of the spherulite radius, $R(t)$, during the isothermal crystallization was observed by the polarized optical microscope (Olympus BH-2) equipped with TV video recording system. The spherulite growth rate, G, was obtained by the slope of $R(t)$.

Results and Discussion

Figure 1 shows typical examples of the time variation of the spherulite radius. A linear increase in R is seen in a wide time regime; i.e., the linear growth of spherulite is observed for neat PVDF and also PVDF/PMMA blends. The growth rate defined by the slope of linear $R(t)$ decreases dramatically with mixing PMMA. When the molecular weight of PMMA, M_2, is large, G in the blend is low. G is lower at the higher crystallization temperature.

We discuss, first, the temperature dependence of G, second, the molecular weight dependence of G, and then, the composition dependence.

Regime Transition. We discuss the temperature dependence of the crystallization rate on the basis of the Hoffman-Lauritzen theory:[5]

$$G \propto \underbrace{\beta_g}_{\text{mobility}} \exp\underbrace{\left(-\frac{K_g}{T_c(\Delta T)f}\right)}_{\text{secondary nucleation}} \quad (1)$$

where β_g is the mobility term which describes the transportation rate of crystallizable molecules to the growth front, T_c is the crystallization temperature, ΔT is the supercooling temperature ($=T_m^\circ - T_c$, T_m° being the equilibrium melting temperature), f is the correction factor given by $2T_c/(T_m^\circ + T_c)$, and K_g is the nucleation constant which depends on the crystallization regime: regime I, single nucleation; regimes II and III, multiple nucleation.[5,6] The value of K_g in regimes I and III is twice that in regime II.

Figure 2 shows the T_c dependence of G in neat PVDF and 55/45 PVDF/PMMA blends. The log G versus $(T_c(\Delta T)f)^{-1}$ plots consist of two straight lines, suggesting

* To whom correspondence should be addressed.

0024-9297/91/2224-4446$02.50/0

Table I
Polymer Specimens

polymer	$M_w \times 10^{-4}$	grade	supplier
PVDF	7.0	KF1000	Kureha Chemical Industries Co.
PMMA	1.3	GI-630	Sumitomo Chemical Co.
PMMA	3.5	GI-634	Sumitomo Chemical Co.
PMMA	11.0	Acrypet M001	Mitsubishi Rayon Co.
PMMA	22.0	GI-633	Sumitomo Chemical Co.
PMMA	36.9		Aldrich Chemical Co.
PMMA	55.0	GI-628	Sumitomo Chemical Co.
PMMA	93.0	GI-625	Sumitomo Chemical Co.

[a] GPC calibrated with standard polystyrene.

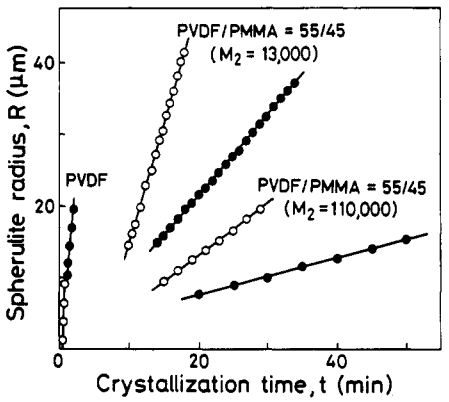

Figure 1. Typical examples of the time variation of the spherulite radius: (○) 147 °C and (●) 152 °C. M_2: molecular weight of PMMA.

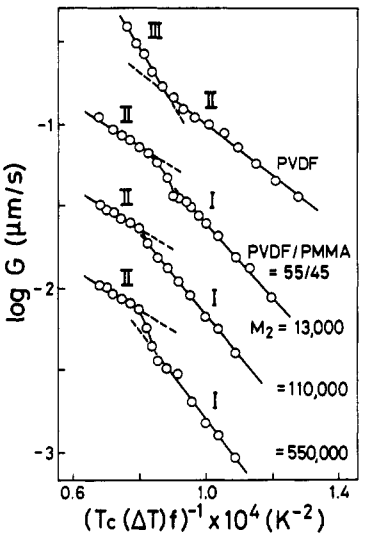

Figure 2. log G versus $(T_c(\Delta T)f)^{-1}$ plots for neat PVDF and three 55/45 PVDF/PMMA blends with different molecular weights of PMMA (M_2). The equilibrium melting temperatures used in this analysis are from ref 7, being estimated by the Hoffman–Weeks plot.

a regime transition as T_c varies. The slope increases by a factor of 2 in the blends with increasing $(T_c(\Delta T)f)^{-1}$, while it decreases by a factor of 2 in neat PVDF. Then, the transition in the blends may be classified as being from II to I, while that in neat PVDF is classified as being from III to II, as T_c increases. Anyway, the results suggest that the crystallization regime in the blends differs from that in the neat polymer system at the same $T_c(\Delta T)f$. A systematic change in the crystallization regime with blend composition at a fixed $T_c(\Delta T)f$ will be discussed later (Figure 4).

Most interesting is the abrupt drop in G at around the regime transition temperature, T_r, in the blends. The gap

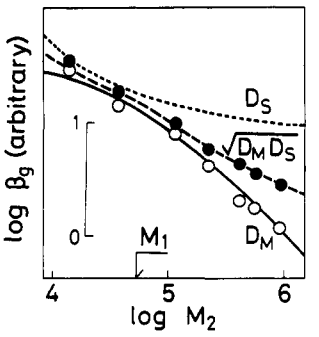

Figure 3. β_g (chain mobility term) versus M_2 (molecular weight of PMMA): (○) regime I (152 °C) and (●) regime II (142 °C). Solid line was calculated by eq 9, dotted line by eq 10, and broken line by eqs 8–10, assuming $D_1°/D_2° = 2$, $\gamma = 0.5$, $n_e = 125$.

of G depends on M_2, i.e., the gap is large for small and large M_2 (1.3×10^4 and 55.0×10^4), while it is small for intermediate M_2 (11.0×10^4). This may be ascribed to the change in the mobility term at T_r, as discussed in the next section.

Two-Step Diffusion Mechanism. Figure 3 shows the M_2 dependence of the mobility term at two different crystallization temperatures locating in regimes I (152 °C) and II (142 °C). The values of β_g were estimated by subtracting the secondary nucleation term, $\exp[-K_g/(T_c(\Delta T)f)]$, from the overall G. β_g exhibits a strong M_2 dependence in regime I but a weak dependence in regime II. The results may suggest that the diffusion mechanism in regime I is different from that in regime II.

Basically, the diffusion process has been described to consist of two elementary processes: the deposition of the first stem on the growth front ("secondary nucleation process") and the attachment of following stems in the chain on the crystal surface ("surface spreading process").[5,6] According to the Hoffman–Lauritzen theory, G is mostly governed by the rate of secondary nucleation, i, in regimes I and III, while it is governed by both i and the rate of surface spreading, g, in regime II:

$$G \propto i \quad \text{for } i/g \ll 1 \text{ (regime I)} \tag{2}$$

$$G \propto (ig)^{1/2} \quad \text{for } i/g \sim 1 \text{ (regime II)} \tag{3}$$

$$G \propto i \quad \text{for } i/g > 1 \text{ (regime III)} \tag{4}$$

where i consists of β_g and $\exp[-K_g/(T_c(\Delta T)f)]$ and g consists of β_g. We define the diffusion coefficients in the surface nucleation process and the substrate completion process by D_M and D_S, respectively. Assuming the β_g is proportional to the diffusion coefficient, i and g may be given by

$$i \propto D_M \exp\left(-\frac{K_g}{T_c(\Delta T)f}\right) \tag{5}$$

$$g \propto D_S \tag{6}$$

From eqs 2–6, we obtain

$$\beta_g \propto D_M \quad \text{(regimes I and III)} \tag{7}$$

$$\beta_g \propto (D_M D_S)^{1/2} \quad \text{(regime II)} \tag{8}$$

In the neat crystalline polymer system, it has been assumed that there is no distinction between D_M and D_S.[5,6] However, in the blend of crystalline and amorphous polymers, the situation should be different. It may be due to the exclusion of amorphous polymer from the crystal

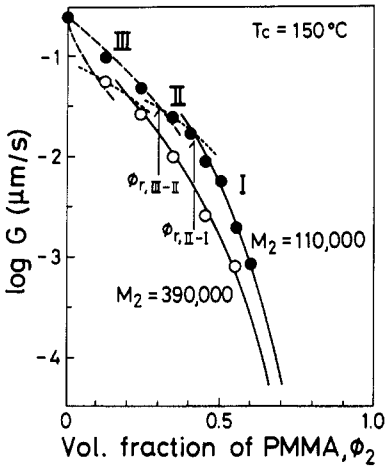

Figure 4. log G versus volume fraction of PMMA: (●) M_2 = 110 000, (○) M_2 = 390 000. Solid lines were calculated by eq 12 (regime I), dashed lines by eq 13 (regime II), and broken lines by eq 12 (regime III).

growth front. That is, the secondary nucleation should be controlled by the competitive two rate processes: the attachment of crystalline polymer onto the crystal surface and the exclusion of amorphous polymer from the surface. The competitive situation could be characterized by mutual diffusion. On the other hand, the surface spreading may be controlled by the rate of the pull-out of residual segments in the crystalline chain from the melt near the growth front. It could be characterized by self-diffusion, as in the neat system.

Brochard et al.[8] have formulated the mutual-diffusion coefficient in the binary blend of polymers 1 and 2:

$$D_M \propto \left(\frac{\phi_1}{D_1^\circ/n_1} + \frac{\phi_2}{D_2^\circ/n_2}\right)^{-1} \tag{9}$$

where ϕ is the volume fraction, D° is the diffusion coefficient of the monomer unit, and n is the degree of polymerization. Equation 9 claims that the mutual diffusion is mostly governed by the slower moiety ("slow theory"). On the other hand, the self-diffusion coefficient in the blend has been formulated by Skolnick et al.:[9]

$$D_S \propto \frac{D_1^\circ}{n_1}\left[\frac{\gamma + (1-\gamma)n_1/n_2}{\gamma + (1-\gamma)n_1 + n_1/n_e}\right] \tag{10}$$

where γ is a constant and n_e is the degree of polymerization between the entanglement points.

Assuming polymer 1 is PVDF and polymer 2 is PMMA, the M_2 dependence of β_g was calculated by eqs 7 and 9. The result is shown by the solid line in Figure 3. The strong M_2 dependence of β_g, observed in regime I (open circles), is nicely explained. The M_2 dependence of β_g in regime II, calculated by eqs 8–10, is shown by a broken line in Figure 3. The weak M_2 dependence observed (closed circles) is successfully described. As a reference, the M_2 dependence of β_g ($\propto D_S$) by eq 10 is shown by the dotted line in Figure 3.

As indicated in Figure 3, there is a gap between the values of D_M and D_S. The gap increases as the difference in molecular weight between PMMA (M_2) and PVDF (M_1) becomes larger. Hence, the larger mismatch in molecular weight yields the larger gap in β_g between regimes I and II, so that the larger gap in G between the two regimes is expected at fixed $T_c(\Delta T)f$. This is the interpretation of the abrupt change in G at the regime transition and its M_2 dependence in Figure 2.

Thus, by taking into account the two-step diffusion mechanism in the crystallization, i.e., the secondary nucleation process governed by mutual diffusion and the surface spreading process governed by self-diffusion, one can interpret (i) the strong and weak M_2 dependences of β_g in regimes I and II, respectively, (ii) the abrupt change in G at T_r, and (iii) the M_2 dependence of the gap in G between regimes I and II at T_r.

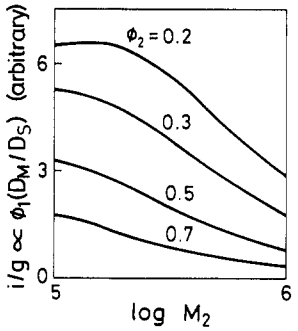

Figure 5. Calculated curves of i/g as a function of M_2 (molecular weight of PMMA) at various compositions ϕ_2 by eqs 9, 10, and 14.

Modified Hoffman–Lauritzen Theory. Sofar, we have omitted a prefactor, ϕ_1, in formulating the secondary nucleation rate. Since i is proportional to the number of crystallizable molecules at the crystal surface,[5,6] which is proportional to the volume fraction of crystalline polymer, ϕ_1, eq 5 should be revised as

$$i \propto \phi_1 D_M \exp\left(-\frac{K_g}{T_c(\Delta T)f}\right) \tag{11}$$

Then, we obtain a modified Hoffman–Lauritzen equation for the polymer blend:

$$G \propto \phi_1 D_M \exp\left(-\frac{K_g}{T_c(\Delta T)f}\right) \quad \text{(regimes I and III)} \tag{12}$$

$$G \propto \phi_1^{1/2}(D_M D_S)^{1/2} \exp\left(-\frac{K_g}{T_c(\Delta T)f}\right) \quad \text{(regime II)} \tag{13}$$

where D_M and D_S are given by eqs 9 and 10, respectively.

Figure 4 shows the composition dependence of G in two systems with different molecular weights of PMMA (M_2 = 11.0×10^4 and 39.0×10^4) at a crystallization temperature (T_c = 150 °C). G decreases with increasing the volume fraction of PMMA, ϕ_2. In the low M_2 systems, the ϕ_2 dependence of G cannot be described by a monotonic curve. It may be reasonable to assume two regime transitions from III to II and from II to I as ϕ_2 increases and set up three curves as shown in Figure 4. The three curves are calculated ones: broken and solid curves by eq 12 and dotted one by eq 13. One sees that the closed circles are nicely located on the calculated curves. Following the procedure, three curves are similarly set up for the open-circle plots (in the high M_2 system).

Note that the above regime assignment is consistent with the results in Figure 2; i.e., regime III at ϕ_2 = 0 (neat PVDF) and regime I at ϕ_2 = 0.45 (55/45 blend) at T_c = 150 °C [$(T_c(\Delta T)f)^{-1}$ = 0.82 for neat PVDF and $(T_c(\Delta T)f)^{-1}$ = 0.96 for 55/45 blends].

In Figure 4, the regime transition compositions, $\phi_{r,III-II}$ and $\phi_{r,II-I}$, in the low M_2 system are larger than those in the high M_2 system. As discussed before, the regime transition takes place due to the change in the relative magnitude of i versus g; i.e., the regime changes from III to II and then to I as i/g decreases. From eqs 6 and 11,

the ratio i/g in the blend is given by

$$i/g \propto \phi_1(D_M/D_S) \exp\left(-\frac{K_g}{T_c(\Delta T)f}\right) \quad (14)$$

The calculated curves of i/g at a fixed $T_c(\Delta T)f$ are shown in Figure 5, as a function of M_2 for various compositions. i/g decreases as ϕ_2 and/or M_2 increases. It suggests the regime transition III → II → I takes place as ϕ_2 and/or M_2 increases. This is the interpretation of the regime transition III → II → I with increasing ϕ_2 and the effect of M_2 on the transition composition ϕ_r in Figure 4.

Conclusion

Various aspects of the crystallization kinetics in the PVDF/PMMA blends were nicely explained by the modified Hoffman–Lauritzen theory involving a two-step diffusion mechanism, i.e., mutual diffusion for the secondary nucleation process and self-diffusion for the surface spreading process. The two-step diffusion mechanism would be applied for unsolved problems, such as the nonlinear time variation of the spherulite growth in polymer/diluent systems[10-12] and the formation of the "open" spherulite in polymer blends.[10]

Acknowledgment. The series of PMMA specimens were kindly supplied by Dr. Masahiko Moritani, Sumitomo Chemical Co., Ltd.

References and Notes

(1) Wang, T. T.; Nishi, T. *Macromolecules* **1977**, *10*, 421.
(2) Ong, C. J.; Price, F. P. *J. Polym. Sci., Polym. Symp.* **1978**, *63*, 59.
(3) Alfonso, G. C.; Russell, T. P. *Macromolecules* **1986**, *19*, 1143.
(4) Briber, R. M.; Khoury, F. *Polymer* **1987**, *28*, 38.
(5) Lauritzen, J. I.; Hoffman, J. D. *J. Appl. Phys.* **1973**, *44*, 4340.
(6) Hoffman, J. D. *Polymer* **1983**, *24*, 3.
(7) Morra, B. S.; Stein, R. S. *J. Polym. Sci., Polym. Phys.* **1982**, *20*, 2243.
(8) Brochard, F.; Jouffroy, J.; Levinson, P. *Macromolecules* **1988**, *16*, 1683.
(9) Skolnick, J.; Yaris, R.; Kolinski, A. *J. Chem. Phys.* **1988**, *88*, 1407.
(10) Keith, H. D.; Padden, F. J., Jr. *J. Appl. Phys.* **1964**, *35*, 1270.
(11) Goldenfeld, N. *J. Crystal Growth* **1987**, *84*, 601.
(12) Okada, T.; Saito, H.; Inoue, T. *Macromolecules* **1990**, *23*, 3865.